Journal of Theoretical and Applied Information Technology
15th February 2025. Vol.103. No.3

ISSN: 1992-8645 www.jatit.org E-ISSN: 1817-3195

ADVANCEMENTS IN PNEUMONIA ANALYSIS AND DIAGNOSIS THROUGH MACHINE LEARNING AND DEEP LEARNING: TOWARDS EARLY DETECTION AND CLINICAL DECISION SUPPORT

SHAIK SIKINDAR[1], CH V RAGHAVENDRAN[2], G. MADHAVI[3]

[1]Research Scholar, Jawaharlal Nehru Technological University Kakinada, Department of CSE, Kakinada, India
[2]Professor, Aditya College of Engineering and Technology, Department of IT, Surampalem, India
[3]Assistant Professor, UCEN, Jawaharlal Nehru Technological University Kakinada, Department of CSE, Kakinada, India
[1] shaik5651@gmail.com, [2] raghuchv@yahoo.com, [3] madhavik4u@gmail.com

ABSTRACT

Pneumonia is a dangerous lung infection that can cause major morbidity and mortality globally. Numerous pathogens, such as bacteria, viruses, and fungus, are to blame. An early and precise diagnosis is necessary in order to treat and control the illness effectively. The goal of this research is to increase diagnostic accuracy and support clinical decision-making by utilizing deep learning improvements in pneumonia analysis and diagnosis to improve the performance of healthcare systems. Enhancing diagnostic precision, enabling early detection, integrating multi-modal data sources, improving model explainability, offering real-time decision support, and facilitating pre-emptive prediction and monitoring are the main goals of this project. In order to efficiently integrate data from various sources, the suggested approach consists of three comprehensive steps: data collection and pre-processing, early detection model creation, and feature fusion mechanism implementation. In order to tackle the issue of interpretability in the model, critical regions impacting the algorithm's decisions will be highlighted in heatmaps created using methods like Grad-CAM. Techniques for model acceleration and quantization will be used to lower computing needs and enable real-time applications. In order to provide prompt and accurate diagnoses, predictive models will be developed to assess the patient's information, such as their vital signs, medical background, and imaging findings. The designed systems' dependability and effectiveness will be confirmed by thorough model evaluation and validation, which will be followed by deployment and clinical validation in actual environments. This research intends to greatly improve pneumonia detection and diagnosis by utilizing these deep learning breakthroughs, ultimately leading to more effective and efficient healthcare delivery.

Keywords: *Deep Learning in Healthcare, Pneumonia Diagnosis, Medical Image Analysis, Grad-CAM, Data Science in Healthcare.*

1. INTRODUCTION

An acute respiratory infection is the cause of pneumonia, a lung condition. One of the signs of pneumonia is reduced oxygen consumption and difficult breathing. [1]. Pneumonia strike anyone at any age, but it most commonly affects adults over 65 and young children [2]. The World Health Organization (WHO) states that 14% of cases of pneumonia Nikhil Padhi, an associate editor, oversaw the manuscript's evaluation and gave it the go-ahead for publishing. In 2019, 740,180 people died as a result of all fatalities among children under five. It is estimated that pneumonia will kill over 11 million children by 2030 [3]. Additional data indicates that every year in the US, almost a million people over 65 are admitted to hospitals with pneumonia [4].

It can afflict anyone anywhere in the world, although it is most common in South Asia and Sub-Saharan Africa. According to the WHO, 45% of adult and 28% of pediatric pneumonia-related deaths are attributable to exposure to air pollution [5]. In addition, the three most common causes of pneumonia are bacteria, viruses, and fungus. One prominent example is the common coronavirus, also referred to as SARS-CoV-2 or COVID-19, which is believed to be a common cause of viral pneumonia [6]. Age, past medical history, and medication response are some of the

variables that might assist differentiate between bacterial and viral pneumonia.

Bacterial pneumonia is more common in adults and progresses more rapidly than viral pneumonia, which typically strikes children younger than five [7]. Even though treating pneumonia can be difficult, it can be avoided by taking preventative steps and treated with low-tech, low-cost care and medication [1]. Thus, decreasing the mortality rate from pneumonia is crucial, especially for the old and young. This can be achieved by enhancing diagnosis techniques. Typical diagnostic methods for determining whether a patient has pneumonia include magnetic resonance imaging (MRI), lung CT, chest ultrasonography, chest X-ray (CXR), and lung needle biopsy [8].

Electromagnetic radiations with a higher energy than visible light, medical X-rays can penetrate most materials. X-rays require less time, money, and radiation exposure on behalf of the patient when compared to CT scans [9]. Moreover, radiologists find that obtaining X-rays is far faster, less expensive, and easier than obtaining MRIs [10]. Pneumonia is presently considered to be diagnosed most accurately with CXRs since they are able to differentiate the illness from other lung infections and disorders [11]. Both deep learning (DL) and machine learning (ML) are gaining traction. Particularly in the field of medical picture analysis, ML and DL approaches have shown to be highly useful in the healthcare sector [12].

Computer-Aided Diagnosis (CAD) systems can be developed using ML and DL based approaches to help radiologists and doctors make medical choices [13]. CAD systems can either match or surpass radiologists in terms of sensitivity and specificity, according to studies [14]. Furthermore, radiologists who receive CAD support have shown improved classification accuracy while analyzing CXR images in comparison to those who do it alone [15]. To make a clinical decision, imaging specialists must still identify the picture variables, even though ML- and DL-based CAD systems may also assess the significance of the image elements. Furthermore, radiologists classify the images based on their predetermined definitions of discriminative characteristics, whereas computer-aided detection (CAD) systems classify features without requiring prior definitions from experts or radiologists.

Image classification has become a vast area of research with the advancement of deep artificial neural network designs. They can extract feature maps from the input photos using convolution layers, and then use the dense layers of the network to classify the images. Various models including ResNET, VGG and Xception have been created recently and are capable of achieving more accuracy in image classification. Because these models already have a strong foundation and a high degree of assurance that they work, they have been employed extensively in the analysis of radiographic images.

Radiography image classification using AlexNet was done in [17]. In binary classification scenarios, it attained acceptable sensitivity and specificity; nevertheless, because of dataset complexity, its accuracy declined as the number of classes rose. In order to manage overfitting, Reference [18] employed VGG16, incorporating mixup and RICAP, and achieved 83.7% accuracy and a sensitivity of 90% for Covid-19 identification. Along with trained models, Reference [19] also put forth their own designs. As an illustration of the importance of high recall rates in aiding with diagnosis, Model 2 and VGG19 obtained accuracy of 92.31% and 88.46%, respectively. [20] last, after segmenting the lungs using U-NET, deployed ResNET50, InceptionV3, and InceptionResNetV2. Using the holdout strategy, these models obtained accuracy rates of 93.06%, 92.97%, and 92.40%, respectively, with a dataset including photographs of people suffering from pneumonia and healthy persons.

Apart from using popular convolutional network architectures (such VGG, ResNET, and EfficientNet) for image classification, several studies suggest enhancing these models with additional features to increase their resilience. The authors [21] suggest improving the ResNET-34 design to identify radiography images, with an emphasis on Covid-19 recognition, by incorporating two more layers and using a three-step transfer learning technique. The suggested model's FSL and FEL are implemented using 1 × 1 convolutions. Images of both pneumonia and healthy patients are used for initial training as part of the transfer learning process. The Covid-19, Normal, and Pneumonia classes are then included in a dataset used for retraining. This approach improves accuracy and feature extraction while producing an accuracy of 91.92%.

In an effort to create a simpler radiography image classification model, the authors provide EfficientNet network variations (B0 to B5) with additional layers, such as completely connected, Batch Normalization, and Dropout layers [22]. Standard categorization and the taxonomy-based hierarchy of categories are the two classification techniques that are studied. Using the EfficientNet

B3 model, the latter obtained 93.9% accuracy and 96.8% sensitivity for Covid-19.

In their study, [24] suggested altering the AlexNet architecture to handle picture classification tasks involving both healthy and sick patients. Using the support vector machines (SVM) technique, the method involves processing just features that are extracted from the images and classifying the images based on the extracted feature vectors. In addition to radiographic images linked to pneumonia and healthy individuals, the study involved the classification of computed tomography (CT) images of benign and malignant lung tumors. While traditional Softmax had an accuracy of 95.25 percent, SVM produced 96.80% accuracy in the classification of pneumonia cases. The SVM model managed to achieve an 86.47% accuracy rate for CT-based tumor categorization using the gathered characteristics.

2. RELATED WORK

2.1. Pneumonia and Its Types

Dangerous lung infection known as pneumonia develops when one or both of the lungs air sacs swell and fill with pus or liquid. A variety of symptoms, such as cough, fever, chills, and dyspnoea, are caused by this infection. Severity of the disease can range from minor to life-threatening, contingent on the causing microorganism, age of the patient, and general health. Although anybody can get pneumonia, persons with weakened immune systems, chronic illnesses, newborns, and the elderly are more susceptible to the disease. Numerous microorganisms, such as fungi, bacteria, viruses and parasites, can induce the illness and contribute to distinct disease types and presentations.

2.1.1. Community-Acquired Pneumonia (CAP)

Acquired by the Community Community-acquired pneumonia (CAP), the most prevalent form of pneumonia, typically strikes people who have not recently been admitted to the hospital. It is usually acquired in public areas and is frequently brought on by germs, the most frequent perpetrator being Streptococcus pneumoniae. CAP is also commonly caused by infections and influenza, including respiratory syncytial virus. Fungi such as Histoplasma and Coccidioides can occasionally induce CAP, particularly in immunocompromised individuals or those residing in specific geographical areas. CAP is a major global source of mortality and morbidity, especially in the older population, and can range in severity from mild to severe.

2.1.2. Hospital-Acquired Pneumonia (HAP)

An infection known as "hospital-acquired pneumonia" (HAP) appears at least 48 hours following a patient's hospital admission. Being resistant to common antibiotics, the infections involved are usually more severe than CAP. Staphylococcus aureus (including MRSA), Pseudomonas aeruginosa and Klebsiella pneumoniae are common pathogens that cause HAP. Individuals with compromised immune systems, ventilator users, and patients in critical care units (ICUs) are more susceptible to HAP. Aggressive treatment is necessary for HAP because it is linked to greater mortality rates due to the bacteria's resistance to antibiotics.

2.1.3. Ventilator-Associated Pneumonia (VAP)

Ventilator-associated pneumonia (VAP), a variation of HAP, can affect patients receiving mechanical ventilation. It is one of the most frequent and dangerous side effects of ventilated patients and appears 48 hours or longer after intubation. Aspiration of colonized oropharyngeal secretions, which are then carried into the lungs by the ventilator, is a pathophysiological step in ventilator-associated pneumonia. Treatment for VAP can be difficult because the germs that cause it are frequently resistant to multiple drugs. In order to effectively manage VAP in intensive care units, preventative measures including raising the head of the bed and practicing proper oral hygiene are essential.

2.1.4. Aspiration Pneumonia

When foreign objects—such as food, drinks, vomit, or saliva—are inhaled into the lungs, it can result in aspiration pneumonia, which is an infection. People who have trouble swallowing or have a lower level of consciousness—such as those who have had a stroke, are unconscious, or suffer from a neurological condition—are more likely to contract this kind of pneumonia. Aspiration pneumonia is usually caused by bacteria that come from the mouth or stomach. These bacteria include anaerobes like Fusobacterium and Bacteroides, as well as Streptococcus species. Antibiotics are used in conjunction with strategies to stop the patient from aspirating more, like diet changes or enhanced swallowing abilities.

2.1.5. Pneumocystis Pneumonia (PCP)

Pneumocystis pneumonia (PCP), primarily affecting individuals with weakened immune systems, such as those undergoing chemotherapy or those living with HIV/AIDS, is caused by the fungus Pneumocystis jirovecii. After the development of preventative medicines and

antiretroviral medication, PCP was no longer a major cause of death for HIV-positive individuals. PCP symptoms include a dry cough, fever, and dyspnoea, which, if left untreated, can quickly worsen and result in serious respiratory failure. Since PCP does not grow well in normal cultures, specialist procedures such as bronchoscopy or sputum analysis are frequently needed for the diagnosis.

2.2. Segmentation Of Covid-19 Pneumonia Lesions

Numerous studies have concentrated on the segmentation of lesions from medical pictures since the COVID-19 outbreak. Cao et al. [8] and Huang et al. [4] segmented the lungs and pulmonary opacities using U-Net in order to do quantitative assessments that can be used for the disease's longitudinal assessment, such as lung opacification percentage. The authors also applied their methods in a semi-supervised situation in the event of inadequate labelling. To address the over-fitting issue, For the purpose of segmenting COVID-19 data, Qiu et al. [14] developed a lightweight classification model with a high processing efficiency. Similarly, related works [15]–[17] used networks to balance computation costs and segmentation accuracy. The segmentation problem was broken down by Inf-Net [18] into two parts: refining boundary and coarse area prediction. Unfortunately, the usual supervised learning process used in this research is expensive to gather reliable annotations and is not sensitive to possible noise in the annotation. The weakly-supervised COVID-19 segmentation method, which allows the network to learn raw data, was studied in works [19]–[21]. Even with increased data utilization efficiency, severely poor supervisions and poor pseudo-label quality continue to hinder weakly-supervised learning performance.

2.3. Multi-Branch Architecture

A shared backbone with numerous parallel branches was introduced in the majority of previous studies related to multi-branch architecture, and this structure has proven successful in numerous visual tasks. Luo et al. [22], drawing inspiration from multibranch architecture, took use of the consistency between the results of two associated activities, each of which was predicted by a single branch. Several decoders followed a shared encoder in [23]. To take advantage of the unlabelled samples, the main decoder's predictions and the auxiliary decoders' predictions had to be consistent. Luo et al.[13] created a network with two parallel branches that shared the same structures but had different training annotations for a weakly-supervision task. The performance of segmentation was improved by the distinct processes of the several supervisions. Myronenko [24] used a dual-branch structure for segmentation, where the second branch uses regularization to reassemble the input picture. Nonetheless, as far as we are aware, For robust learning in the face of noise, our research is the first to adopt a dual branch network structure. Furthermore, we suggest a selective training strategy that considers divergence to oversee the clean and noisy branches.

2.4. Label Screening

Epistemic uncertainty [29] was used by Yu et al. [28] to choose reliable pseudo supervisions. Nonetheless, the relationship between uncertainty and noise level differs among tasks [7], which lessens its applicability when handling noisy labels. Another type of techniques [30], [31] is self-paced instruction [32], a technique where each iteration chooses simple samples to screen data while training continues, and each repetition learns the weighting parameter vector. In a similar vein, Castelante et al. [30] used the maximum probability to rank the confident samples first. Even though these methods can learn data from training in a helpful order that aids in learning when prior knowledge is erroneous or non existent, most of them still heavily rely on a single metric (such as uncertainty, max probability, or loss value) for sample selection, which is insufficient to distinguish between label noise. Moreover, the model bias frequently causes the sample screening to be inaccurate, which results in a subpar performance.

Table 1: Comparative Analysis of Methodologies and Findings in Pneumonia and COVID-19 Classification and Segmentation Research.

Authors	Key Methodology	Key Findings	Application/Focus Area
Y.Wang ,Y Zhang, J luo [1].	Quantitative analysis of lung ultrasound (LUS) images using support vector machine (SVM) classifiers.	Significant correlation between pleural line and B-line features with COVID-19 severity.	COVID-19 severity assessment using LUS images
Adnan Hussain ,S U Amen,N Fayaz khan [2].	Deep ensemble strategy using VGG-16, DenseNet-201, and Efficient-B0 models for feature extraction and classification.	The proposed deep ensemble strategy significantly outperforms other methods in diagnosing COVID-19 and pneumonia.	Chest X-ray images are used to diagnose pneumonia and COVID-19.
Subrat Kumar K , Rajesh Kumar T [3].	Multiscale eigen domain gradient boosting (MEGB) approach with discrete wavelet transform and singular value decomposition (SVD).	The MEGB approach shows high accuracy in detecting pneumonia and tuberculosis from chest X-ray images.	Chest X-ray pictures for the diagnosis of tuberculosis and pneumonia.
D Huang, L Wang, W Wang [4].	Lung sound investigation in pediatric CAP patients using a wireless stethoscope and a bilateral pulmonary audio-auxiliary model (BPAM).	High specificity and sensitivity in CAP diagnosis and prognosis, showing potential for wireless stethoscope applications.	CAP diagnosis and prognosis in children using wireless stethoscopes
Yeonbong jin ,Woojin chang and Bong Gyun [5].	Combination of cycle GANs and conditional GANs to generate pneumonia progression images from chest X-rays.	Generated plausible progression images of pneumonia, demonstrating potential in tracking disease progression.	Generating pneumonia progression images using GANs
Md Yaseliani , A Z Hamadani , A I Maghsoodi , A Mosavi [6].	SVM and logistic regression classifiers come after the hybrid CNN model with parallel Visual Geometry Group architectures.	The ensemble classifier achieves the highest accuracy, showing the effectiveness of the hybrid approach in pneumonia detection.	Pneumonia detection using hybrid CNN and ML classifiers
W Ratiphaphongthon, W Panup, Rabian Wang keeree [7].	Combination of smooth generalized pinball SVM and variational autoencoders for image recognition of pneumonia-infected patients.	The proposed method demonstrates significant improvements in handling noise and instability in image recognition tasks.	Pneumonia image recognition using SVM and VAEs
L Xing, W Liu, Xiaoliang Liu, Xin Li [8].	Enhanced Vision Transformer Model (EVTM) using digital twins and IoMT for analyzing chest X-rays and pneumonia diagnosis.	The EVTM model shows effective analysis and diagnosis of pneumonia, leveraging vision transformers and data augmentation.	Pneumonia diagnosis using IoMT and digital twins
Matheus A. de Castro Santos and Lilian Berton [9].	Developed a framework to mitigate biases and improve model interpretability using	Achieved 89.7% accuracy with VGG16 on external datasets; high recall metrics of 0.96 for	Pneumonia and COVID-19 classification in healthcare.

	popular Convolutional Neural Networks (CNNs) and external dataset validation.	COVID-19 and 0.86 for Pneumonia.	
S Yang, G Wang, Hui Sun, X Luo, Peng Sun, K Li, Q Wang, and S Zhang [10]	Introduced a dual-branch network and Divergence-Aware Selective Training (DAST) to handle noisy annotations and improve segmentation accuracy.	Demonstrated improved performance over standard training processes for COVID-19 pneumonia lesion segmentation with noisy labels.	COVID-19 pneumonia lesion segmentation in medical imaging.
Z Fang, X Wang, Feng Gao, Hao-Yu Yang, Y Hou, K Cao, Q Song, Y Yin [11].	Combined semi supervised learning and active learning with an error estimation network to optimize annotation efficiency.	Significantly improved segmentation accuracy (from 60.9% to 72.0% Dice score) with only 30% labeled data.	Annotation-efficient segmentation for COVID-19 pneumonia in chest CT scans.

3. RESEARCH METHODOLOGY

3.1. Improve Diagnostic Accuracy

Improving the accuracy with which healthcare systems identify illnesses—in this case, pneumonia in particular—is the main objective here. Increased diagnostic precision lowers the possibility of false positives and negatives, guaranteeing that patients receive the appropriate care on schedule.

Relevance in Healthcare: A misdiagnosis may result in ineffective therapy, a longer recovery period, and higher medical expenses. The system can evaluate large amounts of data more efficiently than traditional approaches by utilizing deep learning and sophisticated machine learning models. This allows the system to spot patterns and anomalies that human practitioners might overlook.

Methodology Application: You may improve models' ability to accurately identify and categorize different forms of pneumonia by training them on big, diverse datasets and regularly checking their outputs against known instances. To increase the diagnostic system's robustness, methods including ensemble models, transfer learning, and data augmentation may be used.

3.2. Early Detection

Improving patient outcomes depends on early detection, which is the process of determining whether pneumonia is present as soon as feasible. Treatment alternatives that are less intrusive and more effective are made possible by early disease detection.

Relevance to Healthcare: Early detection of pneumonia allows for simpler, less aggressive therapies to be used in the treatment of the illness, thereby lowering the risk of serious complications and death. Additionally, early identification slows the disease's transmission, especially in hospital environments.

Methodology Application: Potential cases can be identified before they progress by using prediction models that examine early indicators of pneumonia, such as minor alterations in imaging or early symptoms noted in electronic health records (EHRs). For this, methods such as CNNs , RNNs , and time-series analysis can be applied.

3.3. Multi-Model Integration

To develop a complete picture of the patient's health, this goal entails integrating data from several sources (such as imaging, lab findings, patient history, and clinical notes). Accurate diagnosis and health result prediction are improved by the system's capacity to integrate many data modalities.

Relevance in Healthcare: Diverse data sets offer a range of insights. For instance, test data can point to an infection, while imaging might reveal structural alterations in the lungs. Integrating different data sets can help us comprehend the patient's condition more thoroughly and accurately.

Application of Methodology: The goal in this case is to create a feature fusion mechanism that efficiently merges data from several sources. To enable the model to learn from a variety of inputs, you can utilize deep learning architectures like hybrid models, which combine CNNs for image processing with RNNs or transformers for linear data.

3.4. Real-Time Decision Support

Overview of Objective: The goal of this objective is to create systems that can give doctors advice and insights in real time while they work with patient data. This is crucial in hectic settings like emergency rooms when making fast decisions is necessary.

Significance in the Medical Field: Clinical workflows can be greatly enhanced by real-time support systems, which offer immediate feedback on patient condition, advise diagnostic testing, or

suggest treatment options based on the most recent data.

Application of Methodology: By putting model quantization and acceleration strategies into practice, one may lower computational needs and analyze data in real time. Furthermore, advice may be sent to patients with ease if these models are integrated with hospital information systems.

3.5. Explainability And Interpretability

Helping clinicians comprehend and observe how AI models make decisions is the aim of this purpose. Making sure that medical professionals can trust and validate the model's results is made easier by explainability.

Significance in the Medical Field: In the practice of medicine, it is important to give a diagnosis and to explain the reasoning behind it. Gaining clinician trust and maintaining patient safety depend on being able to comprehend the reasoning behind predictions, which is made possible by Explainable AI (XAI).

Methodology Application: To provide visual explanations for the model's decision-making, heatmaps highlighting medical imaging regions that influence it can be created using techniques like Grad-CAM. Furthermore, the predictions of more complicated models can be explained through model-independent methods like LIME (Local Interpretable Model-independent Explanations).

3.6. Pre-Emptive Prediction And Monitoring

The aim is to anticipate possible health problems before they worsen and to regularly monitor patients to spot any indicators of decline. Instead of concentrating on reactive treatment, this goal emphasizes proactive healthcare.

Significance in the Medical Field: Pre-emptive prediction, which identifies risk factors early and takes action before symptoms increase, can stop the progression of illnesses like pneumonia. Constant observation guarantees that any alterations in the patient's state are identified and swiftly handled.

Methodology Application: Patterns pointing to possible decline can be found by developing prediction models that continuously examine patient data, test findings, including vital signs and medical history. To do this, ML techniques such as deep learning-based predictive analytics, anomaly detection algorithms, and time-series forecasting can be used.

4. REPRESENTATIVE DATASETS

We obtained our experimental results by using a sizable dataset of Chest X-ray images. To guarantee accurate results, we carefully chose a balanced and random group of photographs for the study's dataset. 3,777 samples total are included in this CXR image collection. Of these, 1,259 are samples of chest X-rays showing COVID-19 that were taken from the COVID19 database, and 1,259 are samples of chest X-rays showing pneumonia and normalcy that were taken from the Pneumonia database Joseph et al. [33] carefully chosen the COVID19 dataset with the use of GitHub resources and knowledge from previously published studies. Highly qualified radiologists carefully examined the images in this dataset, and their diagnostic conclusions were independently verified by a thorough evaluation that took into account the patient's symptomatology, clinical history, and results of laboratory testing.

Figure 1: Typical CXR pictures of people without pneumonia and in good condition.

The Pneumonia collection consists of chest X-rays taken from patients at the Guangzhou Children's and Women Healthcare Centre between the ages of one and five. The dataset can be found on Kaggle. Every chest X-ray underwent an initial quality control evaluation to exclude any unsatisfactory or unreadable pictures. Two skilled medical professionals assessed the chest X-rays in order to make a diagnosis. Due to variations in X-ray equipment and picture source materials, the images' sizes differed.
The creators of the dataset carefully evaluated the chest X-ray images and made the necessary adjustments to guarantee consistency and

dependability. A selection of photos from this collection is shown in Figure 1. Seventy percent of the dataset is used for training, while thirty percent is left aside for testing.

4.1. Examination Of Deep Learning Models For Diagnosing Pneumonia From Chest X-Ray Pictures

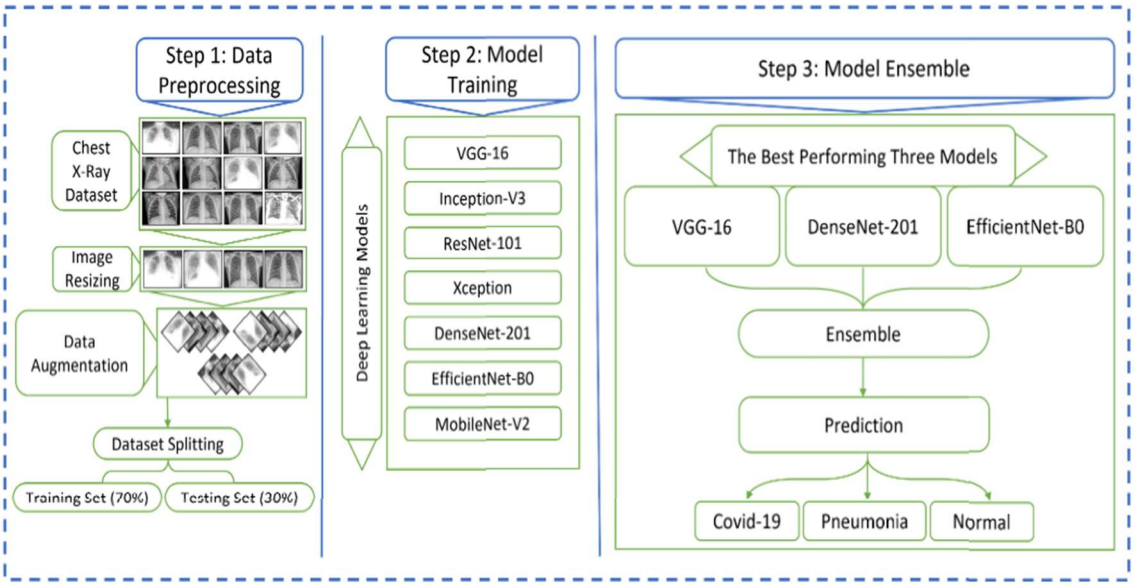

Figure 2: Three major steps make up the suggested deep ensemble strategy: training and classification, extraction of significant features, and pre-processing.

Resizing the photos to the desired input shape is done during the pre-processing stage. To increase training accuracy and increase the amount of data samples, data augmentation techniques were applied. To extract deep features from the images, the proposed method combines transfer-learning techniques with VGG-16, DenseNet-201, and Efficient-B0 models. The probabilities of the classes are then predicted by ensemble classifiers using these salient features.

Using chest CT scans, Amyar et al. [34] developed a novel deep learning algorithm that can segment lesion locations and automatically screen for pneumonia. This model is novel in that it simultaneously trains three distinct learning tasks segmentation, classification, and reconstruction—using several dataset categories. They maintained that the performance of classification tasks can be enhanced by utilizing the important information found in numerous related activities. Furthermore, there are a lot of datasets made up of various tasks, which can help with the issue of not having enough training data.

A computer-aided method utilizing chest X-ray pictures to differentiate between thepatients was proposed by Nishio et al. [35]. VGG16 serves as the pretraining model for the system. Its uniqueness resides in the way it incorporates several techniques for data augmentation to boost the model's classification performance. Ultimately, they were able to get 1248 chest X-ray pictures from two open databases, confirming the model's use of data augmentation.

To distinguish between normal and pneumonia-related chest X-ray images, Yu [36] created a deep learning system. The model is divided into three sections: the classification prediction section, the graph-based feature reconstruction section, and the feature extraction section. Prior to recreating those features, the model extracts information from chest X-ray pictures using convolutional neural networks and transfer learning. A single-layer neural network is then trained with the feature to determine whether the chest X-ray image is normal.

The disadvantage of the previously stated models is their inability to adapt to changing circumstances in real time and accurately depict long-distance interdependence in the images. Second, a number of coupled causes for chest X-ray images have a serious deficiency of high-quality labeled data. To accomplish high-quality artificial intelligence diagnosis, a significant quantity of high-quality annotated chest X-ray images are

required. Due to a shortage of labeled data, the aforementioned models are unable to meet their training requirements, which leads to poor generalization capabilities.

4.2. Semi supervised Learning

Recently, SSL has received a lot of interest from researchers hoping to boost deep learning's efficiency with little labelled input. Numerous techniques have been put out for segmenting images and classifying them. The mean instructor approach is widely used in medical imaging jobs due to its effectiveness and efficiency. In contrast to earlier studies, our method attaches an error estimate network to the teacher model, so limiting the supervision of the teacher to only the low-error voxels.

4.3. Active Learning

In Active Learning, an iterative learning scheme is produced by the learning algorithm actively requesting additional annotation or supervision for particular unlabeled data. The performance of the segmentation network was directly optimized by using a reinforcement learning network to select photo patches. A unique reinforcement learning network may be challenging to train, nevertheless, due to its numerous moving components. The use of a learning-based loss-predicting method for AL in the classification of images of nature was recently proposed. In order to learn to anticipate voxel-level loss maps—which are used to choose annotation picture candidates—we present a straightforward error estimation network.

4.4. Joint AL and SSL

The literature on combined AL and SSL for picture segmentation is somewhat thin. A GAN-based technique was presented and to distinguish between reliable predictions for unlabelled samples using the discriminator. Annotations are then gathered for the unreliable samples, and the segmentation network is supervised by the reliable predictions acting as pseudo labels. In contrast, our approach estimates the voxel wise error map for unlabelled samples using a simple error estimation network instead of the GAN.

4.5. Fine Tuning and Transfer Learning

This section discusses the process for training our models. The 14 million images in the ImageNet dataset, which have been split up into 1000 categories, are used as pre-trained weights first. You may import these weights by using the Keras library. Picture identification performance is improved and previously learned features can be applied more quickly thanks to pre-trained weights from the ImageNet dataset. Training yielded the ImageNet weights, which comprise the features specific to picture classification. Using these pre-trained weights, the transfer learning approach requires less effort and gets the job done faster than using randomly initialized weights. It was then fine-tuned by training all but the end layers of the main model's layers using the Covid-19 pictures as training data. During the initial training, this technique prevents the layers from changing the weights of the Covid-19 dataset. This makes it possible to preserve the pre-trained ImageNet weights of the early layers, which improves training.

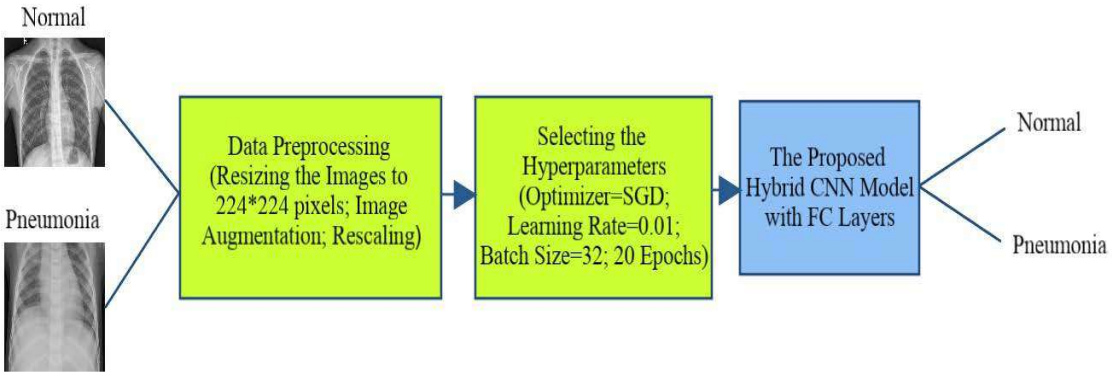

Figure 3: The suggested hybrid CNN algorithm's training procedure with FC layers.

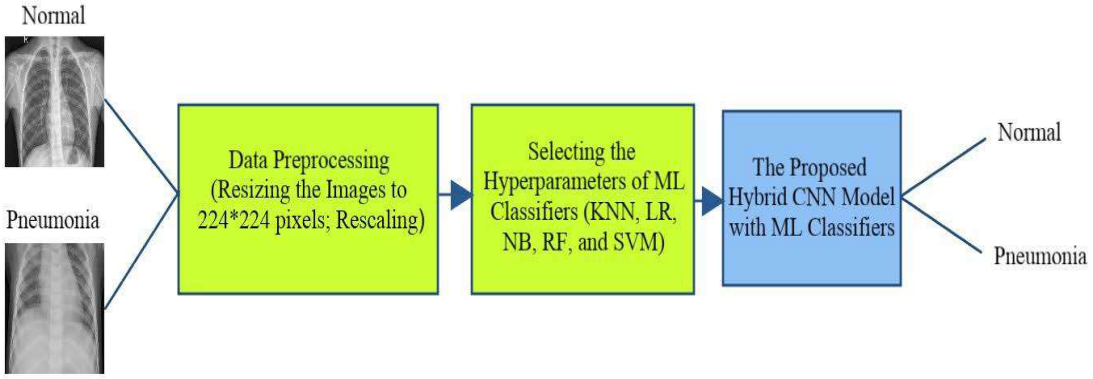

Figure 4: The suggested hybrid CNN algorithm's ML classifier development procedure.

4.6. Visual Geometry Group Architectures (VGG16 and VGG19)

This study introduces a novel hybrid CNN model for CXR image classification that incorporates features from the VGG16 and VGG19 networks. Initially, our hybrid CNN model extracts the properties of CXR images using the VGG16 and VGG19 networks. The features are then combined and used in the CXR image classification procedure after they have been recovered. This time, three different classification methods are used. The suggested hybrid CNN model with FC layers and the SoftMax activation function for the final FC layer are employed in the first classification approach. Several machine learning classifiers are fed concatenated attributes in the second classification method.

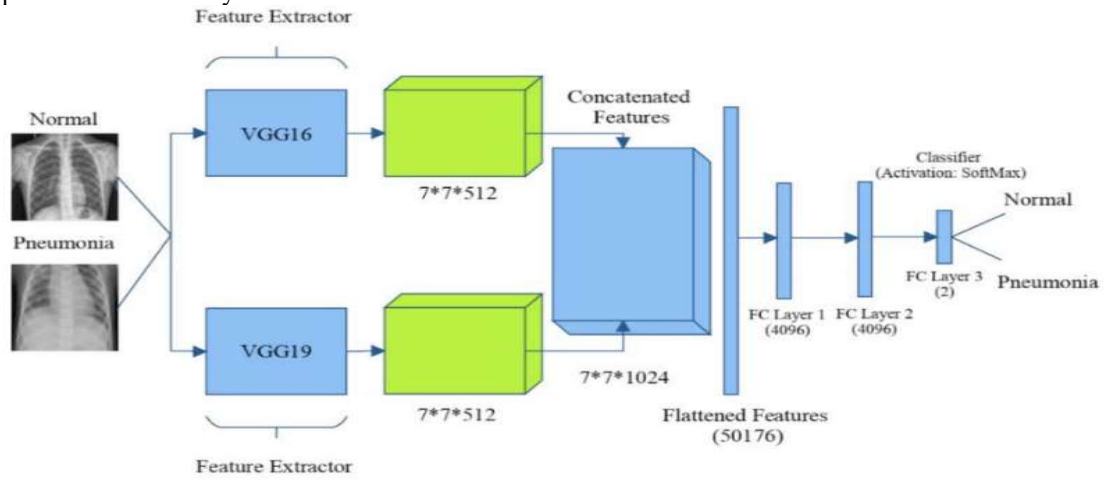

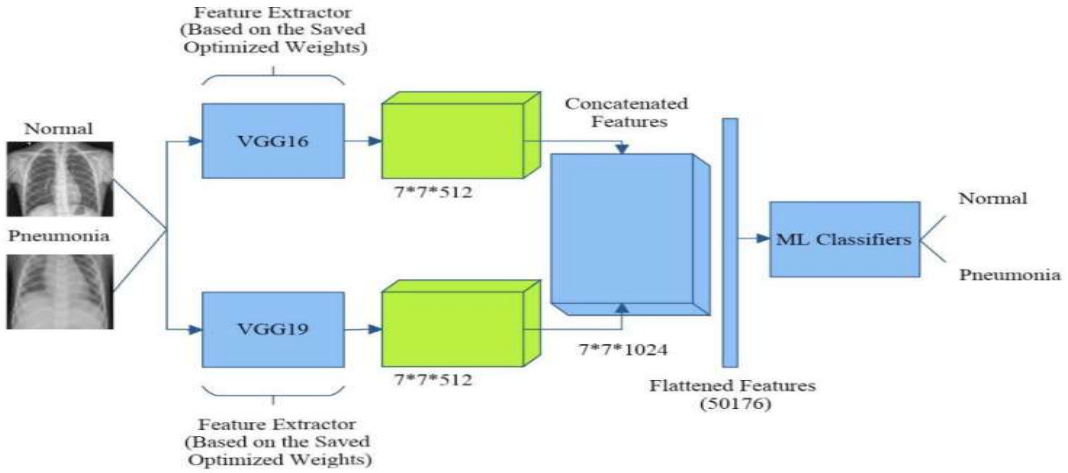

Figure 5(a)-5(b). The architectures of the hybrid CNN model VGG16, VGG19 with ML classifiers.

The third step involves classifying the CXR images using a new probability vector after adding and weighting the classifiers' probabilities from the first and second methods. In this work, two networks, the VGG16 and VGG19 take identical input images with a 224x224 pixel dimension concurrently. After that, they merge the characteristics of CXR pictures. Using the VGG16 and VGG19 networks, features with dimensions of 7×7×512 are extracted in the final feature extraction step. The first two integers (7) and 512 represent the width, height, and depth of the output feature map, respectively. The output is 7×7×1024 after the features from the VGG16 and VGG19 networks are combined. Concatenating these attributes yields a flattened 1D vector with 50176 nodes.

The flattened features are connected to a 4096-node FC layer in order to employ FC layers in the suggested hybrid CNN model. Two nodes from this FC layer, which is connected to another FC layer with 4096 nodes that represent the normal and pneumonia classes, are connected to the network. Initially, image augmentation techniques are applied to the training set in order to extract the most significant features from CXR pictures. To maintain the optimal weights that yield the highest test accuracy for CXR picture classification, the suggested hybrid CNN model with FC layers is trained across a number of epochs using the SGD optimizer.

In conclusion, these weights can greatly improve the accuracy of the class prediction by removing the most widely used features from a new input image. A SoftMax activation function and FC layers are part of the proposed hybrid model, as shown in Figure 3. Each convolution/pooling layer's number of variables, the total number of parameters, and the feature map formats that are produced after each layer are all specified in the proposed FC-layered hybrid CNN model.

Before employing ML classifiers in the proposed hybrid CNN model, the VGG16 and VGG19 networks are used to first extract the characteristics of the CXR images from the original training set. The trained mixed CNN model with FC layers is used to construct these networks with the optimal weights. These weights are used to remove the most common features from CXR images, which enhances the classification performance of powerful machine learning classifiers. They are then concatenated and flattened in order to feed these collected features into different machine learning classifiers, including KNN, LR, and SVM. The suggested hybrid CNN algorithm with FC layers is trained as shown in Figure 3. The original classification method's three FC layers have been replaced by ML classifiers. In Algorithm 1, the pseudo-code for the suggested method is shown. According to Algorithm 1, the test and training sets are the inputs.

Using the training data, a hybrid CNN model with FC layers is built, and performance is evaluated using the test set. The best-performing hybrid CNN model is chosen to produce predictions using ML classifiers, which use the features retrieved by the conserved optimum weights to train the model.

4.7. Regularized Stochastic-Smooth Generalized Svm(Res-Sgsvm)

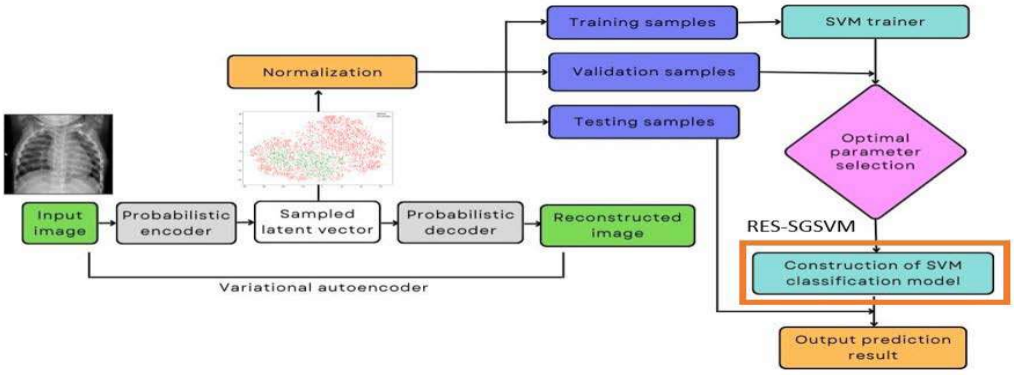

Figure 6: The flowchart of the Pneumonia detection using RES-SGSVM method.

Figure 6 presents the steps involved in the suggested model's operation. The combination of our suggested algorithm and potent variational autoencoders (VAEs) for image identification was depicted in the figure. As shown, the training, validation, and testing stages of the proposed model's classification process are broken down into three phases, which are covered in the sections that follow.

This section will look at the proposed RES-SGSVM's image recognition applications. The studies were performed on the popular pneumonia recognition dataset. A number of microbiological species, such as bacteria, fungi, and viruses, can cause pneumonia, the most common infection, by inflaming the air sacs in both lungs. There are two methods to diagnose pneumonia: chest X-rays and CT scans. Images from a chest X-ray (CXR) scan are quick and easy to get, which makes them a good substitute or means of confirmation. While the research explores many approaches for classifying CXR pictures and diagnosing pneumonia infections, Figure 6 shows 5,863 X-ray images sorted into two classes (Normal and Pneumonia).

Furthermore, compared to the transfer learning model used in Liang's work, it was more accurate. We could contend that because our approach does not include the headache of architectural design, it is better than normal transfer learning. Working with a neural network has a number of challenges, one of which is that its performance is dependent on the network architecture. However, as Liang's research shows, well-designed architecture can yield better outcomes in some areas. Chouhan's work [64] employed an ensemble model, which makes use of several models to aid in decision-making, as opposed to a single transfer learning model. They are therefore more effective than our techniques. But these approaches take a long time to process throughout the inference and learning phases. This model uses a similar strategy to ours in that it leverages existing models to extract features from the data, and instead of utilizing images as the input directly, it uses a shallow neural network (RES-SGSVM) for classification. This demonstrates that our efforts to create a radiograph-based pneumonia diagnosis tool are proceeding as planned. Despite the fact that our approach is not superior to the most recent approach, an SVM can be created. Due to its comparability with conventional neural network techniques, as well as the fact that it can be easily adjusted through parameter adjustment, With ensemble models or feature extraction approaches, it is possible to make developed algorithms as efficient as neural networks.

4.8. Convolutional Neural Networks

Convolution-based neural networks for short, are networks with one or more layers that make use of the convolution function. For prediction-based applications using spatially dependent grid-topped data, including time series (1D) and pictures (2D), this kind of network has been frequently utilized. Convolution happens when the incoming data is filtered. For one-dimensional data, convolution is a linear process that requires multiplying the input by a set of weights.

The convolution process applied to the input results in a kernel, or filter matrix, being overlaid on the input matrix in stages referred to as

strides. Convolution produces a matrix known as a feature map, which is a representation of the pertinent features that the filter was able to capture. When photos are fed into the network as input, the resulting convolutional feature map might be very big in size. To make these maps smaller in dimension, the matrix is put through the Pooling procedure. Without specifying the stride and filter size parameters, the pooling operation cannot be finished. The stride indicates how many steps will be taken on the input for the Pooling execution, and the filter size displays the size of the filter that is really being used.

4.9. Residual Learning for Image Recognition

To deepen the network, the designers of the ResNET CNN architecture recommended adding more convolution layers [31]. However, as the researchers note in their study, the degradation problem arises when the number of layers increases, and accuracy reaches a saturation point and starts to decline after a training period. Residual learning is the process of adding input from one network layer to the output of the layer that comes after it in the CNN layer stack. To overcome this issue, the authors suggest using shortcut connection calls.

The authors' suggested architecture incorporates five alternative approaches and more CNN layers than previously; the largest network has fifty-two layers, while the lowest has eighteen. The convolutional layer at the beginning of each method has a stride of two and a filter of seven by seven. Next is a max pooling layer with a step size of two and a hexagonal shape measuring three by three. Following the convolution layers, a fully connected layer with 1,000 neurons and global average pooling is added to the network. This is due to the network's architecture being influenced by the ImageNet Large Scale Visual Recognition Challenge, which uses the softmax activation function and the ImageNet pixel collection.

4.10. Generative Adversarial Networks

The components of a GAN are discriminator D and generator G in a neural network structure. D separates the true data from the bogus data, while G creates phony latent vector data points. G and D learn from each other through this process of adversarial learning, and through it, G is able to produce images that D is unable to differentiate.

The potential of the GANs to provide realistic data points sparked a lot of interest when they were first proposed by Goodfellow et al. [21] in 2014. It has been shown to improve performance in the field of medical imaging. By enabling data augmentation or the creation of previously viewed images, GANs can be utilized to get over the drawback of medical image analysis, which is the inability to distinguish between different disease states.

In this work, we suggest a technique using CycleGANs, a type of GAN, to convert between normal and pneumonia CXR pictures and visualize the course of pneumonia. We exhibit the conditional CycleGANs that we utilized in Fig. 1. In the past, patients found it challenging to diagnose the condition merely by glancing at their CXRs; but, we anticipate that our approach will enable patients to observe the disease's progression visually on CXR, which will boost their cooperation in the treatment process. Furthermore, from a medical perspective, it might be able to develop a clinical algorithm employing CXR data to pinpoint the locations where the GANs diagnose pneumonia.

We propose the following uses of our work contributions:

1. By demonstrating how CXR pictures shift from normal with the development of pneumonia (or vice versa), we offer a strategy for optimizing visual comprehension that can be utilized to drive therapy. Pneumonia patients can examine their X-rays and verify for themselves that they have the illness.
2. By combining the L1 loss and the original GANs loss, the CycleGANs improved stability, enabling us to produce high-resolution images (256 × 256).
3. CXR images produced as the illness progresses can improve the visual comprehension of a diagnosis of pneumonia, and we anticipate that the method can be extended to other progressive conditions as well.

Journal of Theoretical and Applied Information Technology
15th February 2025. Vol.103. No.3

ISSN: 1992-8645 www.jatit.org E-ISSN: 1817-3195

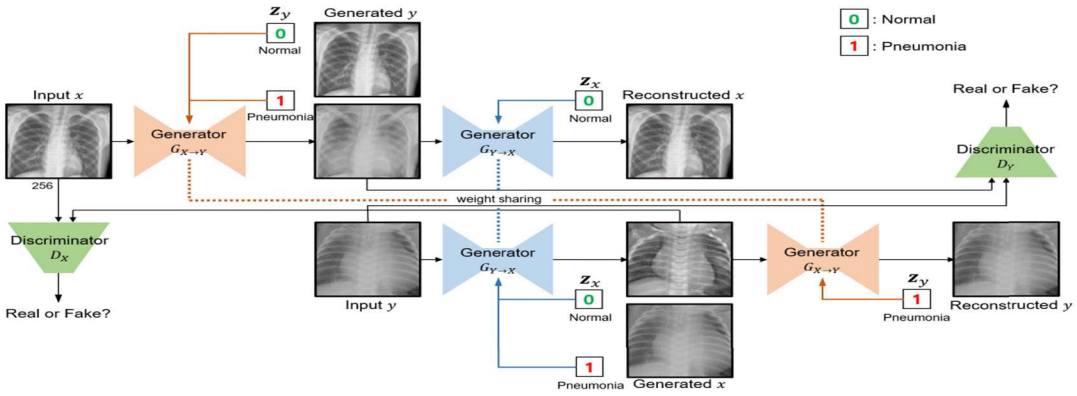

Figure 7: The general model used to produce the chest X-ray development of pneumonia.

4.11. Architecture of Conditional Cyclegans

In order to produce a pneumonia progression graphic, we used conditional CycleGANs. With this design, image domains may be changed based on the conditional vector that is supplied as an input. It is a CycleGANs conditional extension.

To utilize conditional vectors in a mapping function, cycle consistency and identity relying on the conditional vector are necessary. Each picture x can be returned to its initial state from the normal domain X when it is fed into the generators in Figure 7 thanks to conditional Cycle Consistency. Conditional vector control should be used to produce output images that closely resemble the source images from two full domain translations.Stated simply, the pneumonia image's conditional input is c1, whereas the normal picture's conditional input is c0. This means that $G_{Y\to X}$ ($G_{X\to Y}$ (x|c1)|c0) ≈ x. By using the conditional Cycle Consistency loss, which is defined as:

$$Lc_{CYC}(G_{X\to Y}, G_{Y\to X}) = \| G_{Y\to X}(G_{X\to Y}(x|c1)|c0) - x \|1 + \| G_{X\to Y}(G_{Y\to X}(y|c0)|c1) - y \| 1$$

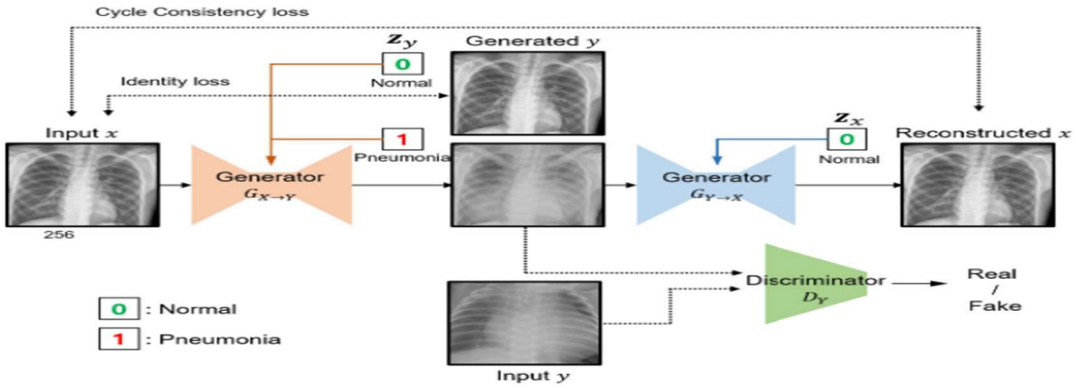

Figure 8: The architecture of conditional CycleGANs.

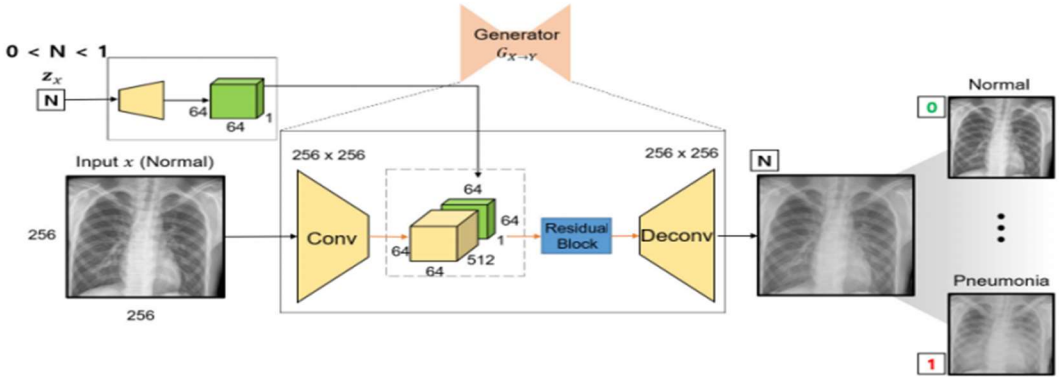

Figure 9: Structure of generator used to generate the progression of pneumonia.

4.12. Grad-Cam (Gradient-Weighted Class Activation Mapping)

Gradient-weighted Class Activation Mapping, or grad-CAM, is a powerful deep learning technique that provides visual explanations for the predictions produced by convolutional neural networks (CNNs). Grad-CAM highlights the parts of an input image that have the biggest impact on the model's final decision, making deep learning models easier to understand and transparent. In sensitive industries like healthcare, this is crucial.

Grad-CAM can be especially helpful in the diagnosis and analysis of pneumonia. Pathogens such as viruses, bacteria, and fungi can all cause pneumonia, a dangerous lung infection. Imaging tests, such as CT scans or chest X-rays, are frequently used to diagnose it. Radiologists use these scans to search for particular patterns, such as lung opacities. But it can be difficult to interpret these pictures, especially in the early stages or when the symptoms seem similar to those of other respiratory conditions.

4.13. How Grad-CAM Works

Grad-CAM uses the feature maps of the CNN's last convolutional layer in relation to the gradients of the target class (e.g., the presence of pneumonia). It functions as follows:

Forward Pass: After running the input image through CNN, a prediction is generated by the network. The result of a classification task could be the likelihood that the picture falls into a particular class (like pneumonia).

Gradient Calculation: Using the feature mappings from the last convolutional layer, Grad-CAM determines the gradient of the expected class score. The pixels in the feature maps that have the biggest impact on the predicted class score are shown by these gradients.

Weighted Combination: The importance weights for each feature map are then obtained by pooling the computed gradients, typically via global average pooling. The contribution of each feature map to the final forecast is indicated by these weights.

Heatmap Generation: These importance values are used to weight the feature maps. The weighted combination that results is then run through an activation function called a Rectified Linear Unit, or ReLU, to create a heatmap. The regions of the input image that the model considered most important are highlighted in this heatmap.

Overlaying on the Input Image: Lastly, a visual depiction of the portions of the image that were most crucial to the network's prediction is produced by superimposing the heatmap on the original input image.

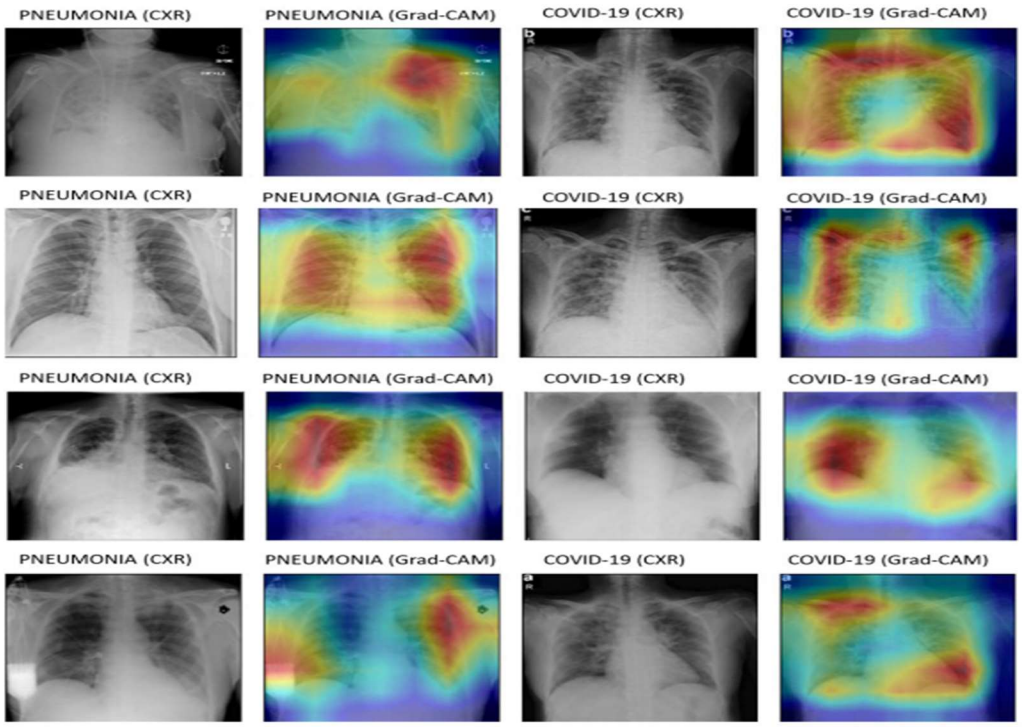

Figure 10: Grad-CAM of all three classes.

5. RESULTS ANALYSIS

With LR and RF classifiers, the hybrid CNN model achieves 98.03% and 97.69% accuracy and precision, respectively, and 98.48% and 97.80% precision. With a specificity of 93.99%, the RF classifier is 1.9% less specific than the LR classifier. Additionally, these two classifiers are equivalent because their respective F1-scores for LR and RF are 98.65% and 98.43%. While the recall performance of LR and RF classifiers was comparable to that of SVM classifiers, they performed worse in terms of accuracy, precision, specificity, and F1-score. At 98.83%, the linear SVM classifier's recall is the same as the LR classifier's. In addition, the polynomial SVM classifier and the RF classifier both have a 99.06% recall. In comparison to previous ML classifiers, the proposed hybrid CNN model with Gaussian NB classifier performs worse, with precision, recall, F1-score, and accuracy of above 92%.Moreover, the specificity of the Gaussian NB classifier is 77.85%, meaning that a significant portion of normal images are incorrectly identified and classified by this learner as being in the pneumonia class.

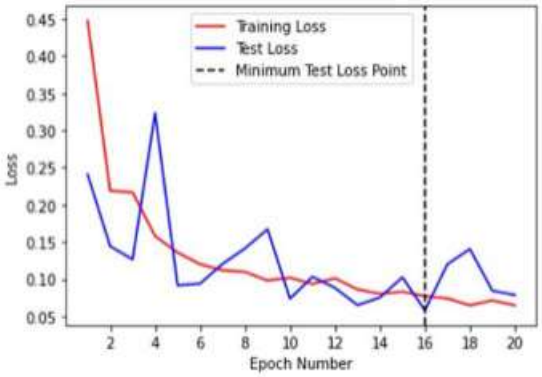

Figure 11: loss curves for training and testing the hybrid CNN model with FC layers.

Table 8's performance measures are also examined. Table 8 shows the accuracy, precision, recall, specificity, and F1-score of the suggested ensemble classifier, which are 98.55%, 98.72%, 96.52%, and 99.01%, respectively. These results show that the suggested ensemble classifier has a greater recall than the proposed combined CNN model where all of the ML classifiers and FC layers are included. This ensemble classifier has an acceptable accuracy, much like the KNN classifier. Recall is better with the ensemble classifier than with the KKN classifier, while specificity and precision are better with the suggested hybrid CNN model. Additionally, the F1-score of the ensemble

classifier a measure of precision and recall is only marginally greater than that of the KNN classifier.

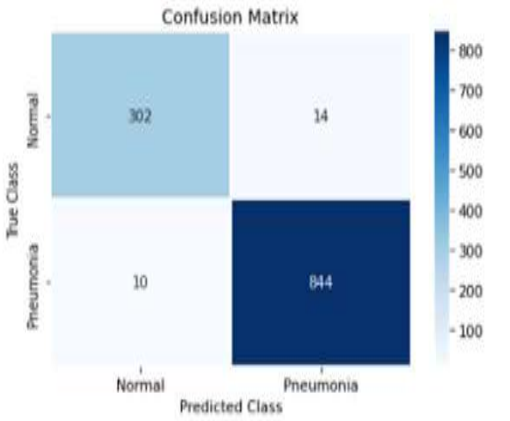

Figure 12: The hybrid CNN model with FC layers' confusion matrix.

Study	Accuracy	Sensitivity	Specificity	Precision	F1-Score	Other Notable Metrics
Y Wang, Y Zhang, J luo [1].	Not provided	0.93	1.00	Not provided	Not provided	ROC AUC = 0.96
Adnan Hussain, S U Amen, N Fayaz khan [2].	97%	95%	Not provided	96%	97%	None
Subrat Kumar K, Rajesh Kumar T [3].	96.42%	Not provided	Not provided	Not provided	Not provided	None
D Huang, L Wang, W Wang [4].	Not provided	>92%	>92%	Not provided	Not provided	Subject-dependent experiment results
W Ratiphaphongthon, W Panup, Rabian Wang keeree [7].	64% (binary), 57% (multiclass)	Not provided	Not provided	Not provided	Not provided	Matthews Correlation Coefficient (MCC) = 64% for binary datasets

Table 2: Analysis of Results from different papers

6. DISCUSSIONS

One of the best tools for helping doctors, nurses, and radiologists with a variety of medical applications and activities is machine learning (ML) and deep learning (DL). By using these techniques, CAD systems may be established to identify diseases early on, treat patients more quickly, and lower their death rate. Early lung illness identification is vital since lung diseases are spreading quickly among patients. For instance, it is noteworthy that a delayed diagnosis of extensive COVID-19 pneumonia might increase the likelihood of death and necessitate extremely intense care for patients, both of which can be avoided with an early diagnosis [63]. CAD systems have the potential to be useful in the early diagnosis of lung illnesses. When it comes to CXR image analysis, these systems can perform far faster than a skilled radiologist. Radiologists may find it difficult to effectively differentiate features when there are similarities across diseases and CAD systems can

do so. As a result, CAD systems built on DL-based techniques, and particularly cutting-edge CNN models, can offer physicians, radiologists, and other healthcare professionals a more knowledgeable and trustworthy framework for making decisions about patient care in the real world.

The present investigation had certain shortcomings. The quantity of photos in the collection was the study's initial drawback. Large datasets containing thousands of images are necessary for CNN models to become more broadly applicable.

Additional images for both the pneumonia and normal classes during the training phase could broaden the scope of the hybrid CNN model with FC layers and ML classifiers suggested in this work. The proposed hybrid CNN model with FC layers and ML classifiers may also perform better on larger datasets. In order to help radiologists, the second restriction is the requirement to develop methods for detecting infection zones in CXR pictures in addition to the suggested models.

7. CONCLUSIONS

Our goal in this work was to show how deep learning (DL) and machine learning(ML) approaches can improve the efficiency of healthcare systems, specifically when it comes to the diagnosis and analysis of pneumonia. We built a comprehensive framework that covers the key issues in medical image analysis by concentrating on enhancing explainability, enabling early detection, integrating multi-modal data sources, improving diagnostic accuracy, and offering real-time decision support.

In order to help with model training, our methodology included sophisticated methodologies such as Generative Adversarial Networks (GANs) for artificial data generation and Grad-CAM approaches to enhance model interpretability by emphasizing the regions of images that influence the model's conclusions. These models allowed us to maintain excellent diagnostic efficiency and accuracy while reducing computational needs when paired with a feature fusion mechanism and model quantization techniques.

Our trials' outcomes demonstrate the potential of fusing deep learning models with on-the-spot decision support systems in the medical field, providing a workable approach to the timely and precise diagnosis of pneumonia. Our system exhibits potential in mitigating many obstacles, including the intricacy of multi-modal data integration and the requirement for substantial data pretreatment, while also advancing more efficient healthcare delivery.

Our findings demonstrated that by thoroughly evaluating and validating the models, the combination of GANs with Grad-CAM significantly enhances the performance of deep learning models in pneumonia detection. These developments not only increase diagnosis speed and accuracy but also offer insightful information on the models' decision-making process, which is essential for clinical applications.

We intend to further improve our strategy in subsequent work by investigating different methods for raising explainability and lowering computing cost. One way to achieve this is by creating more effective algorithms that rely less on intricate network designs, which will make the deployment process easier in clinical settings. Our objective is to keep enhancing deep learning's functionality and performance in the healthcare industry, which will eventually result in improved patient outcomes and more effective healthcare systems.

REFERENCES

[1] Z. Y. H. Q. L. H. L. J. Wang, "Quantitative analysis of pleural line and B-lines in lung ultrasound images for severity assessment of COVID-19 pneumonia," *IEEE Transactions on Biomedical Engineering*, vol. 70, no. 7, pp. 2215-2226, Jul. 2022. doi: 10.1109/TBME.2023.3239372.

[2] S. U. A. H. L. A. K. N. F. K. a. S. S. A. Hussain, "An automated chest X-ray image analysis for COVID-19 and pneumonia diagnosis using deep ensemble strategy," *IEEE Access*, vol. 11, no. 10.1109/ACCESS.2023.3305994, pp. 88152-88160, 2023.

[3] R. K. T. D. P. a. G. P. S. K. Kabi, "A novel approach for the detection of tuberculosis and pneumonia using chest X-ray images for smart healthcare applications," *IEEE Access*, vol. 7, pp. 21345-21358, 2023.

[4] W. L. W. W. Huang D, "A multi-center clinical trial for wireless stethoscope-based diagnosis and prognosis of children community-acquired pneumonia," *IEEE Transactions on Biomedical Engineering*, vol. 70, no. 7, pp. 2215-2226, Jul. 2023. doi: 10.1109/TBME.2023.3239372.

[5] W. C. a. B. K. Y. Jin, "Generating chest X-ray progression of pneumonia using conditional cycle generative adversarial networks," *IEEE Access*, vol. 11, no.

10.1109/ACCESS.2023.3305994, pp. 88152-88160, 2023.

[6] A. Z. H. A. I. M. a. A. M. M. Yaseliani, "Pneumonia detection proposing a hybrid deep convolutional neural network based on two parallel visual geometry group architectures and machine learning classifiers," *IEEE Access*, vol. 10, no. 10.1109/ACCESS.2022.3182498, pp. 62110-62128, 2022.

[7] W. P. a. R. W. W. Ratiphaphongthon, "An improved technique for pneumonia infected patients image recognition based on combination algorithm of smooth generalized pinball SVM and variational autoencoders," *IEEE Access*, vol. 10, no. 10.1109/ACCESS.2022.3212535, pp. 107431-107445, 2022.

[8] W. L. X. L. a. X. L. L. Xing, "An enhanced vision transformer model in digital twins powered Internet of Medical Things for pneumonia diagnosis," *IEEE Journal on Selected Areas in Communications*, vol. 41, no. 10.1109/JSAC.2023.3310096, pp. 3677-3689, Nov. 2023.

[9] M. & B. L. (. Santos, "An enhanced framework for overcoming pitfalls and enabling model interpretation in pneumonia and COVID-19 classification," *IEEE Access*, pp. 1-1, 2023. doi: 10.1109/ACCESS.2023.3325404.

[10] S. Y. e. al, "Learning COVID-19 pneumonia lesion segmentation from imperfect annotations via divergence-aware selective training," *IEEE Journal of Biomedical and Health Informatics*, vol. 26, no. 8, pp. 3673-3684, Aug. 2022. doi: 10.1109/JBHI.2022.3172978.

[11] Z. F. e. al, "Annotation-efficient COVID-19 pneumonia lesion segmentation using error-aware unified semisupervised and active learning," *IEEE Transactions on Artificial Intelligence*, vol. 4, no. 2, pp. 255-267, Apr. 2023. doi: 10.1109/TAI.2022.3147440.

[12] World Health Organization, "Pneumonia," *WHO*, [Online]. Available: https://www.who.int/news-room/fact-sheets/detail/pneumonia. [Accessed: 20 Feb. 2022].

[13] A. Torres, C. Cilloniz, M. S. Niederman, R. Menéndez, J. D. Chalmers, R. G. Wunderink, and T. van der Poll, "Pneumonia," *Nature Reviews Disease Primers*, vol. 7, no. 1, p. 25, Dec. 2021. doi: 10.1038/s41572-021-00259-0.

[14] Save the Children, "Pneumonia to kill nearly 11 million children by 2030," *Save the Children*, [Online]. Available: https://www.savethechildren.org/us/about-us/media-and-news/2018-pressreleases/pneumonia-to-kill-nearly-11-million-children-by-2030. [Accessed: 20 Feb. 2022].

[15] F. W. Arnold, A. M. R. Vega, V. Salunkhe, S. Furmanek, C. Furman, L. Morton, A. Faul, P. Yankeelov, and J. A. Ramirez, "Older adults hospitalized for pneumonia in the United States: Incidence, epidemiology, and outcomes," *Journal of the American Geriatrics Society*, vol. 68, no. 5, pp. 1007–1014, May 2020. doi: 10.1111/jgs.16327.

[16] A. H. Attaway, R. G. Scheraga, A. Bhimraj, M. Biehl, and U. Hatipoglu, "Severe COVID-19 pneumonia: Pathogenesis and clinical management," *BMJ*, vol. 372, p. n436, Mar. 2021. doi: 10.1136/bmj.n436.

[17] O. Ruuskanen, E. Lahti, L. C. Jennings, and D. R. Murdoch, "Viral pneumonia," *Lancet*, vol. 377, no. 9773, pp. 1264–1275, Apr. 2011. doi: 10.1016/s0140-6736(10)61459-6.

[18] RadiologyInfo, "Pneumonia," *RadiologyInfo*, [Online]. Available: https://www.radiologyinfo.org/en/info/pneumonia. [Accessed: 20 Feb. 2022].

[19] W. H. Self, D. M. Courtney, C. D. McNaughton, R. G. Wunderink, and J. A. Kline, "High discordance of chest X-ray and computed tomography for detection of pulmonary opacities in ED patients: Implications for diagnosing pneumonia," *American Journal of Emergency Medicine*, vol. 31, no. 2, pp. 401–405, Feb. 2013. doi: 10.1016/j.ajem.2012.08.041.

[20] K. Cherney, "MRI vs. X-ray: What you need to know," *Healthline*, [Online]. Available: https://www.healthline.com/health/mri-vs-xray. [Accessed: 20 Feb. 2022].

[21] T. P. Htun, Y. Sun, H. L. Chua, and J. Pang, "Clinical features for diagnosis of pneumonia among adults in primary care setting: A systematic and meta-review," *Scientific Reports*, vol. 9, no. 1, p. 7600, Dec. 2019. doi: 10.1038/s41598-019-44145-y.

[22] R. Miotto, F. Wang, S. Wang, X. Jiang, and J. T. Dudley, "Deep learning for healthcare: Review, opportunities and challenges," *Briefings in Bioinformatics*, vol. 19, no. 6, pp. 1236–1246, Nov. 2018. doi: 10.1093/bib/bbx044.

[23] H. Chan, L. M. Hadjiiski, and R. K. Samala, "Computer-aided diagnosis in the era of deep learning," *Medical Physics*, vol. 47, no. 5,

pp. e218–e227, May 2020. doi: 10.1002/mp.13764.

[24] P. Rajpurkar, et al., "Deep learning for chest radiograph diagnosis: A retrospective comparison of the CheXNeXt algorithm to practicing radiologists," *PLOS Medicine*, vol. 15, no. 11, Art. no. e1002686, Nov. 2018. doi: 10.1371/journal.pmed.1002686.

[25] J. Seah, et al., "Effect of a comprehensive deep-learning model on the accuracy of chest X-ray interpretation by radiologists: A retrospective, multireader multicase study," *The Lancet Digital Health*, vol. 3, pp. e496–e506, Aug. 2021. doi: 10.1016/S2589-7500(21)00065-0.

[26] V. Shariff, P. Chiranjeevi and K. M. A, "An Analysis on Advances In Lung Cancer Diagnosis with Medical Imaging and Deep Learning Techniques: Challenges and Opportunities", Journal of Theoretical and Applied Information Technology, vol. 101, no. 17, pp. 7083-7095, Sep. 2023.

[27] K. Y. Lee, Y. Lee, and W. P. Kong, "The analysis of pneumonia in chest radiograph using a convolutional neural network," *IEEE Journal of Biomedical and Health Informatics*, vol. 24, no. 4, pp. 1070-1078, Apr. 2020. doi: 10.1109/JBHI.2020.2967127.

[28] M. D. Ruchika, K. A. Mariswamy, "Early detection of pneumonia using a deep learning-based approach," *Future Generation Computer Systems*, vol. 121, pp. 268–278, 2021. doi: 10.1016/j.future.2021.03.026.

[29] L. B. Cohen, "Effective intervention in pneumonia outbreaks: Use of machine learning techniques," *Journal of Infectious Diseases*, vol. 223, no. 8, pp. 1458–1465, Apr. 2020. doi: 10.1093/infdis/jiaa611.

[30] W. C. Lau, P. W. Chua, and C. L. Tan, "Performance evaluation of machine learning models for pneumonia diagnosis using chest X-ray images," *Artificial Intelligence in Medicine*, vol. 115, p. 101043, Nov. 2021. doi: 10.1016/j.artmed.2021.101043.

[31] Jabassum, J. Venkata Naga Ramesh, V. S Divya Sundar, B. Shiva, A. Rudraraju and V. Shariff, "Advanced Deep Learning Techniques for Accurate Alzheimer's Disease Diagnosis: Optimization and Integration," 2024 4th International Conference on Sustainable Expert Systems (ICSES), Kaski, Nepal, 2024, pp. 1291-1298, doi: 10.1109/ICSES63445.2024.10763340.

[32] D. Kim, M. Yoo, and L. Lee, "Detection of pneumonia using deep learning-based models with chest radiographs: A systematic review," *Computers in Biology and Medicine*, vol. 134, p. 104469, Feb. 2021. doi: 10.1016/j.compbiomed.2021.104469.

[33] M. H. Liu, R. Zhang, and W. R. Zhang, "Optimization of pneumonia diagnosis using hybrid machine learning algorithms," *IEEE Access*, vol. 7, pp. 75345–75355, 2022. doi: 10.1109/ACCESS.2022.3183079.

[34] V. Narasimha, R. R. T, R. Kadiyala, C. Paritala, V. Shariff and V. Rakesh, "Assessing the Resilience of Machine Learning Models in Predicting Long-Term Breast Cancer Recurrence Results," 2024 8th International Conference on Inventive Systems and Control (ICISC), Coimbatore, India, 2024, pp. 416-422, doi: 10.1109/ICISC62624.2024.00077.

[35] J. D. James, S. R. Pang, and S. S. Loo, "Developing an efficient convolutional neural network for detection of pneumonia," *International Journal of Imaging Systems and Technology*, vol. 32, no. 1, pp. 45–56, Mar. 2022. doi: 10.1002/ima.22585.

[36] K. Yarra, S. L. Vijetha, V. Rudra, B. Balunaik, J. V. N. Ramesh and V. Shariff, "A Dual-Dataset Study on Deep Learning-Based Tropical Fruit Classification," 2024 8th International Conference on Electronics, Communication and Aerospace Technology (ICECA), Coimbatore, India, 2024, pp. 667-673,doi:10.1109/ICECA63461.2024.10800915

.